https://doi.org/10.3311/PPci.17229

Periodica Polytechnica Civil Engineering, 65(2), pp. 677–689, 2021

Finite Element Model-based Design of Stiffened Welded Plated Structures Subjected to Combined Loading

Balázs Kövesdi[1*]

[1] Department of Structural Engineering, Faculty of Civil Engineering, Budapest University of Technology and Economics H-1111 Budapest, Műegyetem rkp. 3., Hungary
[*] Corresponding author, e-mail: kovesdi.balazs@emk.bme.hu

Received: 19 September 2020, Accepted: 10 February 2021, Published online: 24 February 2021

Abstract

Resistance calculation of steel bridges with orthotropic plates subjected to combined loading situation (bending moment, shear and transverse forces called as M-V-F interaction) can be challenging for designers due to the interactive stability behavior and combined buckling phenomena. The current EN 1993-1-5 standard provides a design method using analytical design equations checking the pure (bending, shear and patch loading) and interaction resistances separately. This design process is complex in the case of steel bridges, especially for box-section bridges having numerous longitudinal and transverse stiffeners. Finite Element Model (FEM) based design can provide suitable design tools for efficient and accurate resistance calculation of these structure types. However, within the modelling process there are numerous questions to be answered regarding material models and imperfections to ensure required accuracy and safe resistance. A new standard prEN 1993-1-14 is currently under development which will provide design rules to finite element model-based design of steel structures, having the aim to answer the main part of the above mentioned questions and standardize the design process. The current paper discusses and demonstrates the methodology of the FEM based design for welded plated structures. Benchmark example for a Hungarian steel box-section bridge subjected to combined loading situation is presented. Effect of different meshing, imperfection combinations and material models are presented and evaluated in the paper. Efficiency of the numerical model and the obtained resistance on the input parameters are evaluated and design example is given for the application of the FEM based design method.

Keywords

FEM based design, plated structures, imperfections, orthotropic plates, box-section bridges, interaction behavior

1 Introduction

Interacting stability behaviour is one of the most important design resistance check for steel bridges build by incremental launching technique, which is quite a common erection method nowadays. During launching nearly all cross-sections come at least once over a support where a concentrated transverse force, bending moment and shear forces are introduced resulting in buckling problem in the slender web. Designers are provided with analytical design equations given by EN 1993-1-5 [1] where design resistance models are standardized for bending, shear buckling and patch loading separately. The EN 1993-1-5 also includes standardized interaction equations for bending and transverse force (M-F), bending and shear buckling (M-V). However, shear and transverse force interaction (V-F) and a M-V-F combined interaction equations were missing from the previous standard. Therefore, there was no standardized design procedure available in the past to check this important design situation and there were only an extremely small number of research activities on this research field. Braun [2] and Graciano and Ayestarán [3] did large efforts to study the combined loading situation of steel I-girders to determine the M-V-F interaction resistance between 2010–2013. New design interaction equations have been developed for these two design situations by Braun and Kuhlmann, which have been validated for bridge structures by Kövesdi et al. [4–5] in 2014. The new interaction equation is given by Eq. (1):

$$\left(\bar{\eta}_1\right)^{3,6}+\left[\bar{\eta}_3\left(1-\frac{F_{\mathrm{Ed}}}{2V_{\mathrm{Ed}}}\right)\right]^{1,6}+\eta_2\le 1{,}0\,, \tag{1}$$

Cite this article as: Kövesdi, B. "Finite Element Model-based Design of Stiffened Welded Plated Structures Subjected to Combined Loading", Periodica Polytechnica Civil Engineering, 65(2), pp. 677–689, 2021. https://doi.org/10.3311/PPci.17229

where: $\bar{\eta}_1 = \frac{M_{\mathrm{Ed}}}{M_{\mathrm{f,eff,Rd}}}$; $\bar{\eta}_3 = \frac{V_{\mathrm{Ed}}}{V_{\mathrm{bw,Rd}}}$; $\eta_2 = \frac{F_{\mathrm{Ed}}}{F_{\mathrm{Rd}}}$.

$M_{f,eff,Rd}$ is the design plastic moment of resistance of the cross-section consisting of the effective area of the flanges and the fully effective web irrespective of its section class,

$V_{bw,Rd}$ is the shear resistance of the web alone,

F_{Rd} is the design resistance to local buckling under transverse forces,

M_{Ed}, V_{Ed} and F_{Ed} are the acting internal forces.

Another possibility to determine the M-V-F interaction resistance is using Finite Element Model (FEM) based design approach. The EN 1993-1-5 Annex C [1] gave design rules for the numerical model-based design. However, these design rules were not complete, and lot of questions arose during the modelling process and analysis which were not answered by the code. The main points to be clarified in case of welded plated structures were how to (i) proceed model validation, (ii) apply imperfections, (iii) create imperfection combinations, (iv) evaluate the nonlinear analysis and (v) handle safety issues. Another problem with the previous design rules were that they were splitted into diverse parts of the Eurocode which were not always harmonized.

To solve these issues, a new code prEN 1993-1-14:2020 [6] is currently under development. The vision of CEN/TC 250/SC 3 was that rules for FEM based design in Eurocode 3 shall be merged into one document dealing with principles based on the rules given already in EN 1993-1-5 (Plated structural elements) [1] and EN 1993-1-6 (Strength and Stability of Shell Structures) [7]. The scopes of the new prEN 1993-1-14 are the followings: (i) providing rules on the use of finite element analysis and other numerical methods, (ii) verifying ultimate limit states, serviceability limit states and fatigue of steel structures, (iii) define the framework of FEM design methods and specify all the steps of the static design process.

In the current paper the application and interpretation of the design rules of the new prEN 1993-1-14 are presented for the stability analysis of welded steel plated structures in the case of a combined stability problem. Complex design situation of a longitudinally stiffened box-section steel bridge is investigated, resistance against M-V-F interaction is determined representing interactive stability behavior. In the case of numerical model-based design of complex structures the imperfections to be applied are not always evident and there are no exact design rules on how to combine different imperfections. The current paper gives special focus on the imperfections to be applied. Different methods on the application of imperfections (hand defined and eigenmode shape type imperfections) are also presented and their effect on the resistance is determined. Different imperfections representing different stability problems are also combined using imperfection combination rules. Effect of different imperfection combinations on the ultimate behavior and resistance is evaluated and conclusions are drawn for the analyzed structure type. Results of the numerical simulation can be also influenced by the applied material model. Therefore, the effect of different material models is also highlighted in the current paper.

Another focus point of the paper is on the validation and verification of the numerical model, which have not been standardized in the previous Eurocodes. The new prEN 1993-1-14 will regulate this process, however, its application depends on the applied modelling level and analysis type. Therefore, its application needs clarification and explanation. Differences between the validation and verification process are introduced in the paper and an application example is presented in case of numerical design calculations using direct resistance check.

The third focus point of the paper is on the demonstration how to evaluate non-linear analysis and how to determine the design buckling resistance for steel structures. The evaluation of the obtained failure mode and load-displacement diagram is a key issue of the numerical simulations. Application example is introduced, and determination method of the characteristic and design resistance level is presented.

2 Benchmark case description

The analyzed structure is a typical Hungarian box-section girder usually used for large span highway bridges. The cross-section contains longitudinally and transversally stiffened orthotropic plates using closed section longitudinal stiffeners (Fig. 1). The carriageway width is 12.0 m with a sidewalk of 1.315 m at one side of the cross-section and a curbside of 500 mm at the another side. The cross-section depth in the middle of the girder is 4506 mm with 2.5 % deck plate slope in lateral direction. The width of the bottom plate is 5500 mm, the distance between the webs at the location of the deck plate is 7500 mm. The thickness of the deck plate is 14 mm along the entire bridge. Thickness of the web and bottom plates are changing along the length of the bridge, at the analyzed location both plates have a thickness of 12 mm.

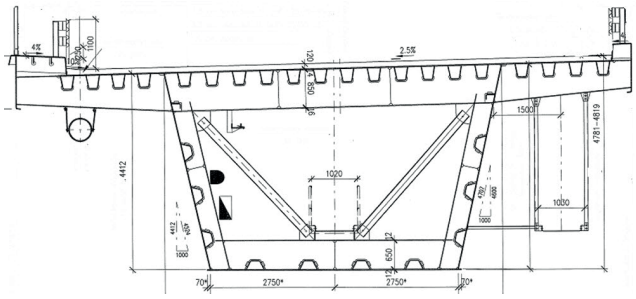

Fig. 1 Typical cross-section of the bridge

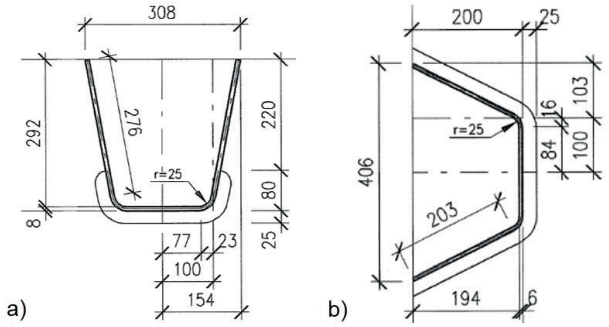

Fig. 2 Geometry of the longitudinal stiffeners: a) on the deck plate, b) on the webs and bottom plate

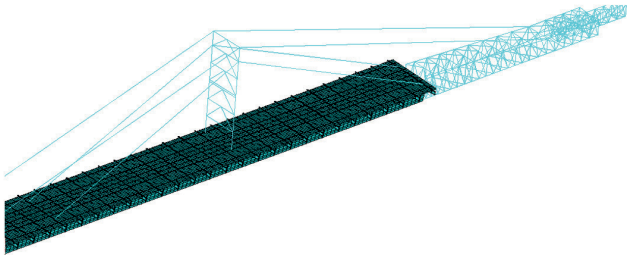

Fig. 3 Global model of the bridge used to model launching process

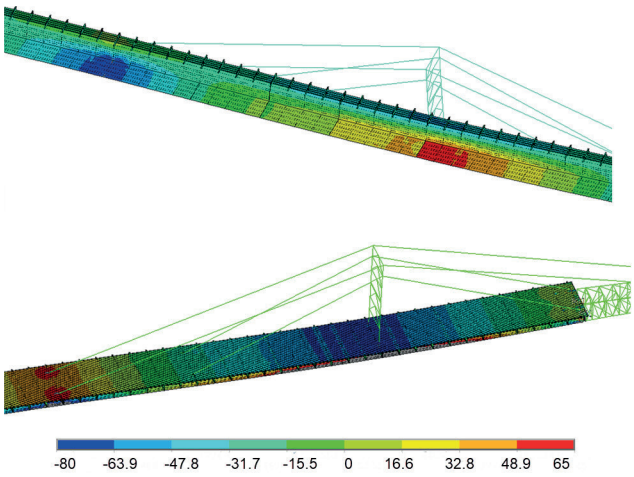

Fig. 4 Normal stresses in the box-section in the critical stage of launching

The deck plate is stiffened by 20 longitudinal stiffeners having closed section as shown in Fig. 2(a). Thickness of these stiffeners is equal to 8 mm and they are placed quasi-uniformly along the width of the deck plate in a distance of 300 mm. Bottom plate is stiffened by using 4 longitudinal stiffeners having the geometry shown in Fig. 2(b) with a thickness of 6 mm. Web plates are stiffened using three different longitudinal stiffeners. The upper stiffener is a steel L-profile having dimensions of 200 × 100 × 8 mm. The lower three stiffeners have the same closed-section geometry as shown in Fig. 2(b), the second and third stiffeners have a thickness of 6 mm, the lower stiffener has a thickness of 8 mm.

Cross-girders support the orthotropic plates at each 4000 mm along the bridge longitudinal axis. All cross-girders have a T-section. The deck cross-girder has a web depth of 850 mm with 10 mm web thickness and a flange of 230 × 16 mm. The web cross-girders have a web depth of 400 mm with 10 mm thickness and a flange of 200 × 12 mm. The cross-girders stiffening the bottom plate have a web depth of 650 mm with 10 mm thickness and the flange size is 200 × 12 mm. Each second cross-girder is additionally stiffened by a V-type bracing system with bracing rods having HEA 200 profiles. The box-section, the main load carrying system is made of S355 steel grade with characteristic yield strength (f_y) of 355 MPa and ultimate strength (f_u) of 510 MPa. The bridge is built by incremental launching process using launching truss and suspension system as shown in Fig. 3 to decrease deflection and negative bending moments at the cantilever stage.

The launching process has been simulated step-by-step within 2.0 m increment. The critical stage during launching is determined on the global numerical model by determining the maximum internal forces and stresses in the flanges and the web, as shown in Fig. 4. The internal forces representing the critical stage on the global model has been applied on the local numerical model used to resistance check.

3 Numerical modeling specialties

3.1 Geometrical model and boundary conditions

The load carrying capacity and the ultimate load of the bridge within the critical launching situation is determined by using FEM based design technique. Local model is developed in a general Finite Element program (Ansys 17.2 [8]) to perform the static check. The applied numerical model is a full shell model using four-node thin shell elements. The local model contains a 16 m long segment of the entire bridge between 4 cross-girders, as shown in Fig. 5. Two end cross-sections are supported, where rigid diaphragms are applied using rigid members connected to a node placed in

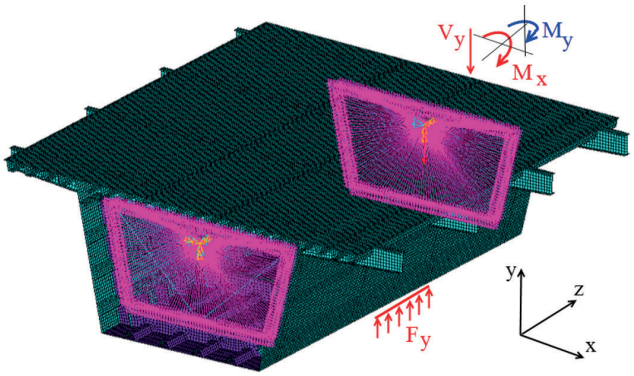

Fig. 5 Local model used for numerical simulation

the centre of gravity of the cross-section. The rigid members link all the 6 DOFs between the coupled nodes. At one end of the segment, the centre of gravity of the cross-section is supported against translations (UX, UY, UZ) and rotations (ROTX, ROTY, ROTZ). At another end the UX, ROTZ DOFs are supported and internal forces (nodal loads – V_y, M_x and M_y acting in the centre of gravity of the cross-section) are applied which intensities are determined from the global model to represent the neglected part of the bridge. At the location of the launching equipment, transverse force is applied at the web-to-flange junction with a loading length (s_s) of 2500 mm. Rigid members are applied along the load introduction place to model the stiffness of the launching equipment (single beam with large bending stiffness) to ensure realistic stress distribution against patch loading. The aim within the definition of the load and support models was to ensure equivalent internal force distribution on the sub-model which occurs on the global model during erection of the bridge. Therefore, the applied boundary conditions in the numerical model are chosen to reflect the behavior of the physical supports and internal forces of the real structure in a realistic and conservative manner.

3.2 Material model

The new prEN 1993-1-14 defines four different standardized material models, as introduced in Table 1. Detailed description of these material models and background information are given in [9]. All the standardized material models are linear elastic – plastic material models with or without strain hardening. The first three models are standardized with predefined characteristics. The fourth model is a test-based material model for numerical simulations usually used to extend laboratory tests. The first three material models are applied and compared in the current analysis to demonstrate their effect on the ultimate behavior of the analyzed structure.

Table 1 Standardized material models for numerical calculations [6]

Model	
with yielding plateau	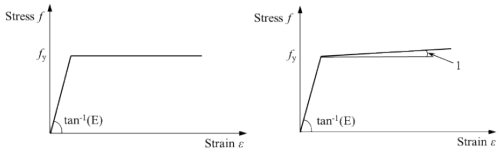 (a) (b) 1 tan-1 (E/10 000)
with yielding plateau and strain hardening	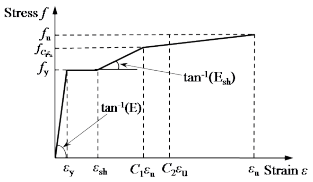 (c)
using measured stress-strain curve	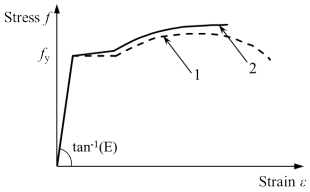 (d) 1 stress-strain curve from tensile test 2 true stress-strain curve

The material models behave linearly elastic up to the yield strength (f_y) by obeying the Hooke's law with Young's modulus (E) equal to 210000 MPa. By exceeding the end of the elastic behavior, the first material model has perfectly plastic behavior without strain hardening. The second model has a nominal plateau slope of E/10000 for numerical stability. In the case of the third material model, yield plateau is modelled according to Eq. (2), and an isotropic hardening behavior defined by Eqs. (3)–(6) are modelled until reaching the ultimate strength (f_u). In the current analysis S355 steel grade is used having nominal values for the yield and ultimate strengths (f_y = 355 MPa, f_u = 510 MPa), respectively.

$$\varepsilon_{sh} = 0.1 \cdot \frac{f_y}{f_u} - 0.055 \text{ but } 0.015 \le \varepsilon_{sh} \le 0.03\,, \tag{2}$$

$$\varepsilon_u = 0.6 \cdot \left(1 - \frac{f_y}{f_u}\right) \text{ but } 0.06 \le \varepsilon_u \le A\,, \tag{3}$$

$$C_1 = \frac{\varepsilon_{sh} + 0.25 \cdot \left(\varepsilon_u - \varepsilon_{sh}\right)}{\varepsilon_u}\,, \tag{4}$$

$$C_2 = \frac{\varepsilon_{sh} + 0.4 \cdot \left(\varepsilon_u - \varepsilon_{sh}\right)}{\varepsilon_u}\,, \tag{5}$$

$$E_{sh} = \frac{f_u - f_y}{C_2 \cdot \varepsilon_u - \varepsilon_{sh}}, \quad (6)$$

where:

$\varepsilon_y = f_y/E$ is the yield strain,
ε_{sh} is the strain hardening strain,
E_{sh} is the strain hardening modulus,
A is the elongation after fracture defined in the relevant material specification (0.2 is used in the current analysis),
C_1 and C_2 are material coefficients.

For S355 steel grade the following values are applied: $\varepsilon_{sh} = 0.015$; $\varepsilon_u = 0.182$; $C_1 = 0.31$; $C_2 = 0.448$; $C_1\varepsilon_u = 0.057$; $C_2\varepsilon_u = 0.082$; $E_{sh} = 2310$ MPa.

This quad-linear material model been proposed to represent accurately the yield plateau and strain-hardening behavior of hot-rolled structural carbon steels, based upon, and calibrated against a large dataset of tensile coupon test results [9]. Only three basic parameters are required for this material model: E, f_y and f_u, which characteristic values are usually known for designers. Application of more advanced material models is also allowed by prEN 1993-1-14, one example is presented by Budaházy and Dunai in [10].

3.3 Imperfections and imperfection combinations

Imperfections included in the FE model should account for the effects of geometric deviations from the perfect shape, residual stresses, and boundary condition defects [6]. Imperfections can be applied by the following two different methods according to [6]:

1. geometric imperfections and additional residual stresses due to fabrication,
2. equivalent geometric imperfections by modification of the perfect shape of the structure; these imperfections are intended to cover the effect of both the geometrical imperfections and residual stresses and have larger magnitudes than solely geometric imperfections.

Version 2 (equivalent geometric imperfections) is applied in the current analysis because application of residual stresses in case of a box-section bridge with longitudinal stiffeners (where the residual stress pattern is extremely complex) is not a realistic design case. If equivalent geometric imperfections are used in a non-linear analysis, imperfections in the form of each investigated failure mode should be adopted. The most detrimental imperfection (that could realistically occur) should be chosen in calculating each potential failure mode. The direction of the imperfection(s) (imperfection combinations) should be chosen to identify the lowest resistance. If the relevant imperfection direction is not evident or defined by other rules, imperfections with different directions should be investigated. If more than one equivalent geometric imperfection form is used, combinations of these forms should additionally be considered.

There are different methods to define equivalent geometric imperfections. The first possibility is the application of imperfection shapes based on predefined standardized functions, or modification of the perfect shape by predefined displacements taken from linear analysis. These standardized imperfection forms represent the commonly observed imperfection shapes after fabrication. The manually defined imperfection shape is often given by a functional description, like sine function, or other functions. Its definition is more complex as for other imperfection types, but usually leads to robust and reliable models. The second possibility is the application of imperfection shape based on linear bifurcation analysis (LBA) corresponding to the eigenmode (shape) associated with the expected failure mode or to a combination of eigenmodes. Eigenmode type imperfections are defined on mathematical bases and the modelling technique is also well clarified. Previous studies proved the application of eigenmode imperfection shape usually leads to safe design. The standard allows using the lowest eigenmode as an imperfection shape, corresponding to the buckling shape of the analyzed panel. If combined stability failure is studied with the numerical model it is also allowed to use the combination of several imperfection shapes representing each possible stability failure modes. In this case all different eigenmodes should be checked and evaluated separately and their combination should be defined depending on their actual shape. Detailed investigation on the combination of different imperfections for longitudinally stiffened plates and simplified application proposal is presented in [11]. The third possibility is the application of the collapse-affine imperfection shapes. The basis of this imperfection shape is a previous GMNIA simulation, where the collapse shape of the analyzed girder is defined, and the original geometry is overwritten by this imperfect shape. This imperfection type is not a commonly used imperfection and currently not allowed by the prEN 1993-1-14, but previous investigations prove their applicability, as presented by Kövesdi and Dunai for patch loading resistance of corrugated web girders [12]. Comparative study on the application of these three imperfection definition modes and their effect on the ultimate load is introduced by Kövesdi et al. in [4] for interacting stability phenomenon for I-girders.

The prEN 1993-1-14 classifies the equivalent geometric imperfections into four sub-groups which are the bases of the imperfection combinations:

1. equivalent geometric imperfections for global structures (e.g., frames),
2. equivalent geometric imperfections for structural members,
3. equivalent geometric imperfections for cross-sections (plates),
4. equivalent geometric imperfections for shell structures.

Where equivalent geometric imperfections arising from different sub-groups are being used (e.g., frame imperfections, member imperfections and cross-section imperfections) each imperfection should be taken with its maximum amplitude and they should be linearly added. For equivalent cross-section imperfections in plated structures, the combination of the imperfections might be necessary. The leading imperfection should be chosen first, with accompanying imperfections at amplitudes reduced to 70 % of the defined value. Each imperfection type in turn should be chosen as the leading imperfection, with the remainder taken as the accompanying imperfections [6]. In the present study two different imperfections are applied, hand-defined imperfections using pre-defined shape considering all possible failure modes (Figs. 6–7) and combination of eigenmode shape imperfections (Figs. 8–10) taken from linear bifurcation analysis (LBA). The maximum amplitudes of the local sub-panel imperfections are taken as min(a/200, b/200) where a and b are the relevant length and width of the analyzed sub-panel. The shape of the local imperfection is a half-sine wave in both directions with a wave length equal by the width of sub-panels. For the global imperfections half-sine wave shape imperfection is applied with a wave length equal by the distance of the cross-girders. The maximum amplitude applied on all longitudinal stiffeners is taken as min(a/400, b/400) where a and b are the relevant length and width of the analyzed panel between the cross-girders.

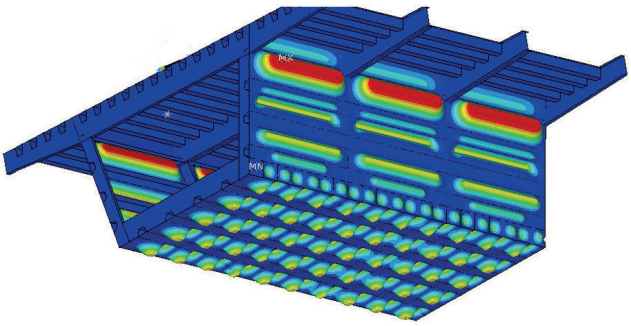

Fig. 6 Local imperfections – buckling of sub-panels

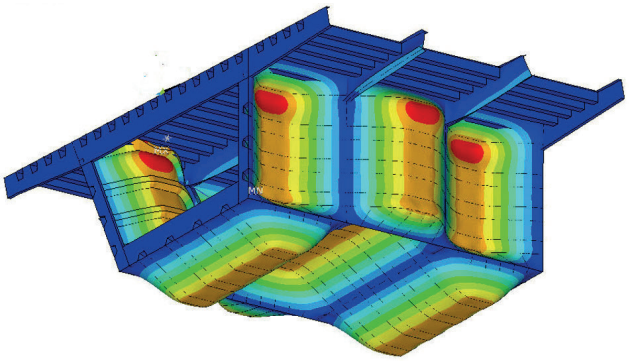

Fig. 7 Global imperfections - buckling of stiffened plate

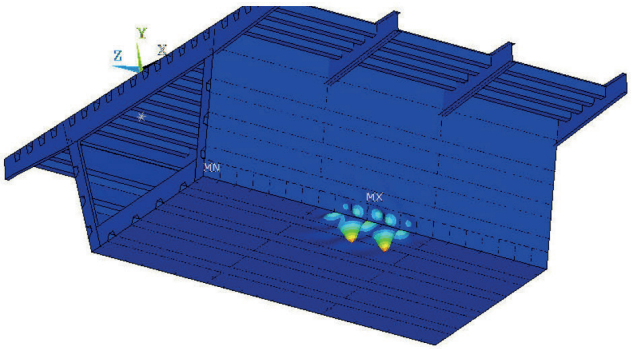

Fig. 8 Eigenmode shape imperfection – mode #1 for local buckling - M-V-F interaction

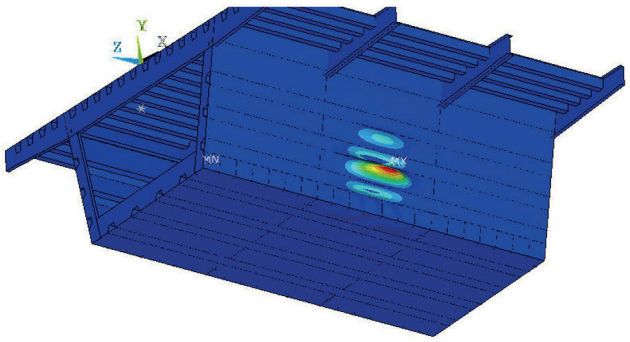

Fig. 9 Eigenmode shape imperfection – mode #3 for sub-panel buckling on the web - M-V-F interaction

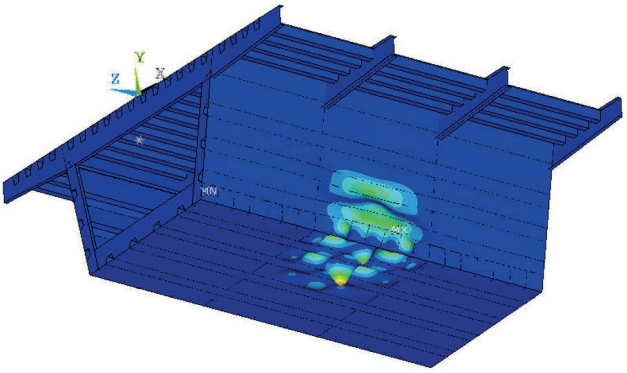

Fig. 10 Eigenmode shape imperfection – mode #4 for global buckling - M-V-F interaction

Eigenmode shape-based imperfections presented in Figs. 8–10 are selected to refer all possible failure modes of the stiffened box-girder. Local buckling type imperfections are covered by the shapes presented in Figs. 8–9 on the web and lower flange. Global stiffener buckling type imperfection on the web plate is covered by the imperfection presented in Fig. 10.

3.4 Analysis type and evaluation strategy

Two types of analysis are carried out on the numerical model: (i) linear bifurcation analysis (LBA) to determine the critical buckling stress and eigenshapes of the investigated box-section and (ii) geometrical and material non-linear analysis with imperfections (GMNIA) to determine the characteristic buckling resistance of the analyzed structure. Result of the non-linear analysis gives the behavior of the structure represented by a load-displacement path related to the chosen boundary conditions and analyzed load case combination considering the effect of elasto-plastic instability. All the relevant load case combinations causing compressive or shear membrane stresses should be accounted for checking the buckling resistance. For each investigated load case combination, a separate GMNIA analysis should be performed. In the current paper the analysis of one load case combination is presented. In the GMNIA the structure should be subjected to the design values of the applied load case combinations increased by a load amplification factor to determine the relevant load-deformation path. Full Newton-Raphson approach is used in the nonlinear analysis with 0.1 % convergence tolerance of the residual force based Euclidian norm. The structural resistance can be determined by the evaluation of the calculated load-deformation path by taking the lowest resistance obtained from the following two criteria C1, C2 (Fig. 11).

1. Criterion C1: the maximum load level of the computed load-deformation path (maximum load or limit load).
2. Criterion C2: the largest tolerable deformation (or strain), where this occurs during the loading path before reaching the limit load.

4 Design resistance check – M-V-F interaction

4.1 Investigated failure mode

Before making a more detailed evaluation the ultimate failure mode of the numerical model is investigated and checked if the applied load and the failure mode are appropriate. Fig. 12 shows the computed failure mode which

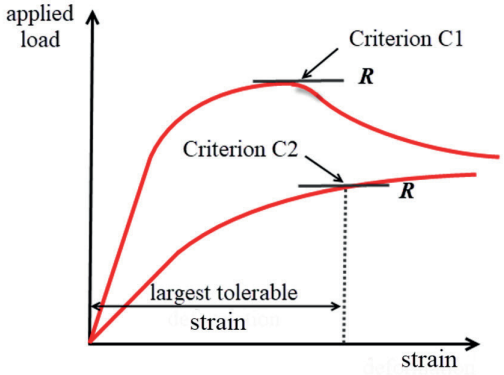

Fig. 11 Evaluation strategy of the load-deformation path

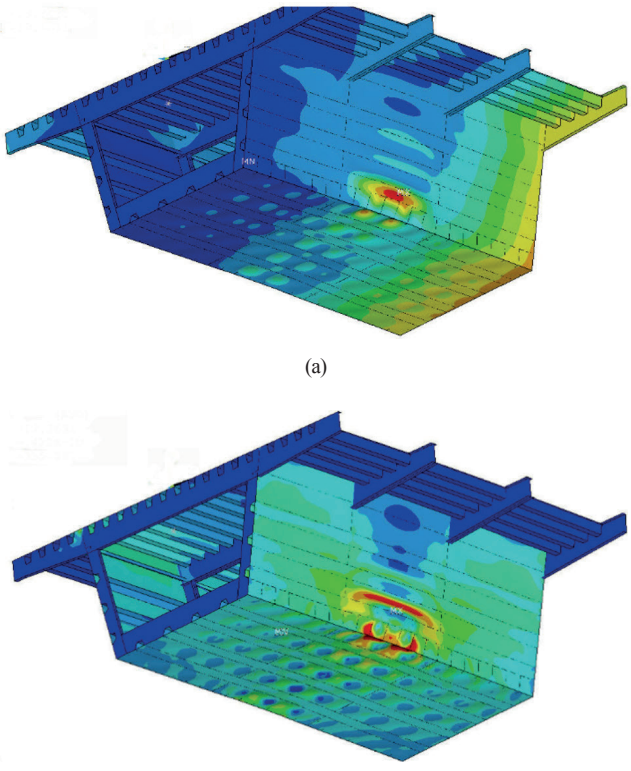

(a)

(b)

Fig. 12 Obtained ultimate failure mode, a) deformed shape, b) von Mises stress distribution at ultimate load level

fits the expectations based on previous experiences. The obtained failure mode is a combined buckling failure of the web under transverse force, shear force and negative bending moment causing compression in the bottom plate.

The buckling failure occurs at the location of the load introduction place of the transverse force within the local sub-panels combined with the global buckling of the lowest longitudinal stiffener of the web. Failure mode also show that the local buckling of the bottom plate sub-panels can be also decisive. In case of structures where buckling failure can happen at different places, the critical location and the most decisive failure mode cannot always be

determined based on the GMNIA analysis. If the resistance of the different structural elements are to be determined, the non-investigated parts could be strengthened, or defined by linear elastic material model, which cannot fail. However, in this case special attention should be given to check if unexpected and intolerable load shedding or load redistribution effects cannot occur.

4.2 Model validation and verification

Validation and verification are important steps of the modelling process, because they demonstrate the applicability and accuracy of the obtained results. However, how extensive validation and verification is necessary in the design praxis depends on the applied modelling level and analysis type. Clear separation between validation and verification will be introduced in the prEN1993-1-14. Verification demonstrates that the numerical solution is a good approximation of the exact mathematical solution and the numerical model is properly used. Verification checks the model sensitivity to discretization and proves the correct application of the numerical model and analysis. Validation is comparison of the numerical results to experimental data or known accurate solutions to demonstrate that the model correctly captures the physical phenomena to be modelled. At first the accuracy of the numerical model, the discretization of the mathematical model and the chosen analysis method should be demonstrated by verification. Validation is the second step comparing the physical behavior and the results of the chosen numerical model or modelling technique. The verification process should include the following checks:

a) discretization error check (mesh density, convergence check),
b) sensitivity check of input parameters,
c) imperfection sensitivity analysis (if relevant),
d) engineering judgement of the calculation results.

Mesh density study should be used to show that the chosen mesh size and element type are accurate for the analyzed problem and the calculation results are not significantly influenced by the discretization. A mesh density corresponding with a 5 % difference with the converged value of the system response quantity is generally expected to provide a good approximation. In the current analysis four-node thin shell elements are applied, which are accurate to model slender plated structures and to analyze buckling phenomenon. Results of the executed mesh sensitivity study is presented in Fig. 13.

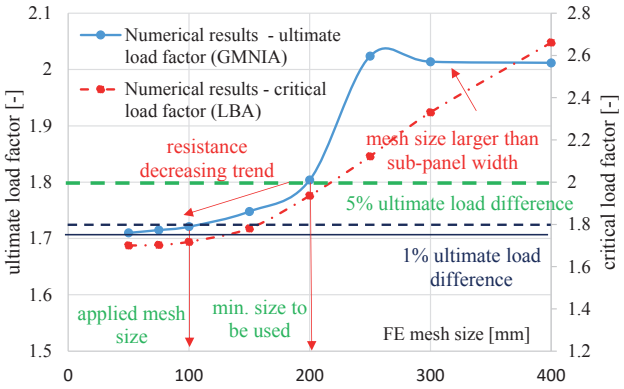

Fig. 13 Result of the discretization error check

Applied mesh size is presented on the horizontal axis, having values between 50 up to 400 mm. The results presented by blue dots and the left vertical axis represents the calculated ultimate load factors based on GMNIA corresponding to the largest load of the load-displacement path where the solver still found convergence.

The right axis and the results marked by red represents the computed critical load factors based on LBA. Results of both system response quantities shows that decreasing the mesh size results in decrease in the ultimate or critical load. The converged value based on the GMNIA results are presented on the diagram. Mesh sizes representing 1 % and 5 % differences to this value are also marked by dashed lines. Based on the discretization error check the minimum FE mesh size should be 200 mm. However, the applied value in the following analysis is taken as 100 mm, which belongs to ~1 % resistance difference to the mathematically correct value. An interesting trend can also be observed on the diagram for a large mesh sizes leading to decreasing ultimate load factor. The reason for it is that ~250–300 mm corresponds to the sub-panel width and for larger element sizes the FE mesh has no further impact on the ultimate load (mesh size is controlled by the panel geometry), however, these calculations can lead to incorrect results. Diagram also shows the difference between the calculated and the mathematically exact solution can be large in case of the ultimate and critical load as well. In the analyzed case the maximum difference in the ultimate load is around 17 %, and 56 % in the critical load factor. These results prove the importance of the discretization error check, because both the ultimate and the critical loads are usually on the unsafe side by applying too large FE mesh sizes. In the presented study the applied shell elements follow the first-order shear-deformation theory (usually referred to as Mindlin-Reissner shell theory).

The element formulation is based on logarithmic strain and true stress measures. The element kinematics allow for finite membrane strains (stretching). However, the curvature changes within a time increment are assumed to be small according to [8].

A sensitivity study involving minor changes to the input parameters determines which data items are crucial to the required SRQ (System response quantity – which is the relevant output value resulting from a certain analysis; it reflects the main objective of the analysis by selecting the major parameters and the limitation of their errors in both validation and verification according to [6]), and shows whether this item must be defined with higher precision or not. This check should be made only for models and input data for which there are no previous experiences or possible sensitivity is raised, therefore it is not presented in the current paper.

Imperfection sensitivity analysis should be only made in case of numerical simulations extending laboratory experiments, where the imperfections have uncertainties. In case of numerical design calculations used for direct resistance check standardized imperfections with predefined magnitudes are applied, which accuracy is proved by researchers. Therefore, no additional imperfection sensitivity should be made.

Engineering judgement should be applied to the results of a calculation. The main characterizing outputs (deformations, internal force, or stress diagrams, etc.) should be checked as presented in Section 4.1.

Validation would be the second step after verification, where benchmark case should be adopted as a reference to check the numerical model and its application in the particular application field. According to prEN 1993-1-14 the highest level of validation is found when using comparison methods in which the numerical results are treated as stochastic variables, with their own input and output uncertainties. Instead of single values for the input and the corresponding result, there are value ranges that can be characterised e.g., by the mean and standard deviation. The result of such a calculation is provided by repeated computations as the inputs are varied according to the estimated probability distributions of the experimental data [6]. The reliability of the numerical model can be also checked via a simplified method by using the model factor (γ_{FE}), which covers the uncertainties of the numerical model and the executed analysis type [6]. In the current investigations numerical model is used, which has been previously validated to test results. If resistance check is applied (check of failure modes with existing Eurocode based design resistance model) using standardized imperfections and if the numerical model is verified as presented here above, simplified model validation can be applied using a predefined value for model factor. The proposed predefined value is equal to $\gamma_{FE} = 1.0$.

4.3 Effect of material models

Non-linear analysis is executed using the same model settings but using three different material models as introduced in Section 3.2. Table 2 gives a summary on the obtained results. The load factors given in the table refers to the load applied on the numerical model in the ultimate loading situation of the bridge during launching (combined loading bending-shear-transverse force interaction). More details on the evaluation and determination of this quantity are given in Section 4.6. Results show the different material models have no significant effect on the ultimate resistance of the analyzed structure. It means the modelling differences of strain hardening has no effect on the obtained buckling resistance. The reason is that the load-deformation path has its maximum value when extreme fibre stresses reaches the yield strength in the middle of the local sub-panels, which is common in case of stability failure modes. It means that the obtained trend is not a general trend, but only valid for this particular design situation checking buckling problems.

The obtained von Mises stresses at the ultimate load level is presented in Fig. 14, showing that maximum stresses are reaching the yield strength in the extreme fiber of panels to buckle causing buckling failure of the girder.

Table 2 Ultimate load factor using different material models

material model	perfectly plastic without strain hardening	perfectly plastic with a nominal plateau slope for numerical stability	quad-linear material model with strain hardening
ultimate load factor	1.737	1.739	1.737

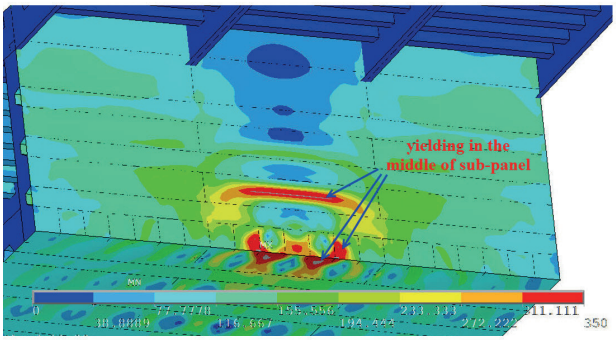

Fig. 14 Von Mises stresses at ultimate load level

4.4 Effect of imperfection combinations

Imperfections can have large effect on the ultimate load level. In case of combined failure modes different imperfections should be combined, as introduced in Section 3.3. The final imperfect shape of the analyzed structure should be obtained by superposition of the equivalent geometric imperfections on the perfect structure covering all possible failure modes and geometric deviations. According to prEN 1993-1-14 in the case of combination of different equivalent geometric imperfections all the possible imperfection combinations (with different signs) should be checked and combination resulting in the smallest resistance should be chosen. It means, many different imperfection combinations are to be investigated in the numerical model, non-linear analysis should be executed to all of them and the minimum resistance is to be selected as final resistance. An example for the imperfection combinations to be checked is presented in Table 3. Three different hand-defined imperfections are combined together using the given combination rules. Global imperfections on the web and bottom plates are handle separately representing the stiffener buckling as shown in Fig. 7. The imperfection direction shown in Fig. 7 is considered as positive for the web as well as for bottom plate. The local imperfection is also considered positive as presented in Fig. 6. However, because the local buckling of the sub-panels is more or less independent from each other, local imperfections are handled separately and no combination rules are applied. All sub-panel imperfections are applied together with positive or negative sign (having alternating directions). The imperfection direction is changed in the load case combination for the local imperfections as well, to find the minimum resistance. Results are presented in Fig. 15 and Table 3, which prove it is important to analyze different imperfection combinations. The difference between the minimum and maximum value for this particular case is 14.5 %. The minimum load factor is equal to 1.734, to be considered for further evaluation.

Results show the direction of the global imperfection has large effect on the ultimate load. Therefore, it is important to perform simulations using both imperfections directions. Results show that resistance is the smallest if the global imperfection on the web panel is taken in the positive direction (shape as shown in Fig. 7). The direction of the accompanying global imperfection on the bottom plate has much smaller effect on the resistance which proves that failure occurs in the web. Results also prove the direction of local imperfections have small effect on the ultimate load.

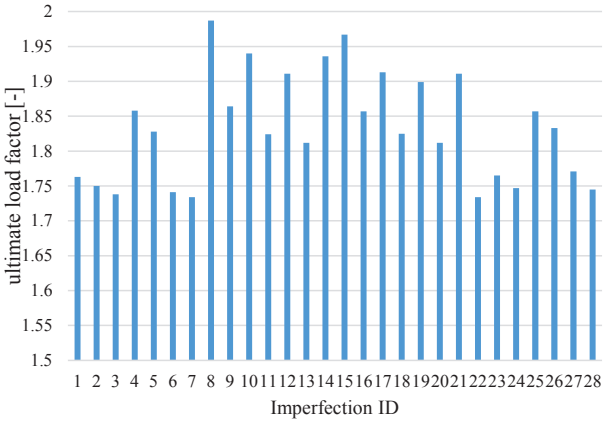

Fig. 15 Effect of imperfection combinations on ultimate load factor

Table 3 Ultimate loads using different imperfection combinations

Imperfection ID	Global imperfections		Local imperfections	Ultimate load factor
	on bottom plate	on web plate		
Imp. 1	+1	+1	-	1.763
Imp. 2	+1	+1	+0,7	1.75
Imp. 3	+1	+1	-0,7	1.738
Imp. 4	+0,7	+0,7	+1	1.858
Imp. 5	+0,7	+0,7	-1	1.828
Imp. 6	+1	+1	+1	1.741
Imp. 7	+1	+1	-1	1.734
Imp. 8	-1	-1	-	1.987
Imp. 9	-1	-1	+0,7	1.864
Imp. 10	-1	-1	-0,7	1.94
Imp. 11	-0,7	-0,7	+1	1.824
Imp. 12	-0,7	-0,7	-1	1.911
Imp. 13	-1	-1	+1	1.812
Imp. 14	-1	-1	-1	1.936
Imp. 15	+1	-1	-	1.967
Imp. 16	+1	-1	+0,7	1.857
Imp. 17	+1	-1	-0,7	1.913
Imp. 18	+0,7	-0,7	+1	1.825
Imp. 19	+0,7	-0,7	-1	1.899
Imp. 20	+1	-1	+1	1.812
Imp. 21	+1	-1	-1	1.911
Imp. 22	-1	+1	-	1.734
Imp. 23	-1	+1	+0,7	1.765
Imp. 24	-1	+1	-0,7	1.747
Imp. 25	-0,7	+0,7	+1	1.857
Imp. 26	-0,7	+0,7	-1	1.833
Imp. 27	-1	+1	+1	1.771
Imp. 28	-1	+1	-1	1.745

Just for comparison purposes load case combinations are also investigated and presented in Table 3 where no combination factors (0.7) are applied, and all local and global imperfections are combined with their maximum

amplitudes (Imp. 6-7, 13-14, 20-21, 27-28). Results prove this situation can lead to the minimum resistance (Imp. 7) without significant conservatism. However, this simplification can lead to much smaller number of imperfection combinations.

4.5 Effect of imperfection definition type

Comparison is made if imperfection combinations of hand-defined imperfections and combination of eigenshapes are applied as equivalent geometric imperfections. The eigenshapes presented in Figs. 8–10 are applied and summarized with their maximum amplitudes. Thus, eigenshapes have directions and geometry coming from bifurcation analysis representing buckling of the analyzed structure, therefore it is expected that eigenmode shape imperfections lead to minimum resistance. The minimum value of the obtained ultimate load factor is 1.734 using combination of hand-defined imperfections as presented in Table 3. If all the three eigenmodes representing local and global buckling failure of the web and bottom plate are applied, numerical calculation results in an ultimate load factor of 1.583. It means that the appropriate application of the eigenmode shapes as equivalent geometric imperfections gives a lower bound approximation of the minimum value from the hand-defined imperfection combinations in this particular case. Calculations are also made using only the first eigenmode shape (Fig. 8) leading to a load factor of 2.12. These results prove even if eigenmode shapes are applied as equivalent geometric imperfections, the application of the first eigenmode shape does not always lead to safe side resistance in case of combined stability failure modes. More eigenshapes representing all possible failure modes should be applied to ensure safe calculation results.

4.6 Result evaluation and resistance calculation

Results of the non-linear analysis is the load-displacement path of the analyzed girder. In the case of the verified numerical model the obtained load-displacement path is presented in Fig. 16. The horizontal axis shows the vertical displacement at the web-to-flange junction in the middle of the load introduction place of the transverse force. Thus, failure occur within the stiffened web above the local load introduction place, therefore this point is selected for evaluation purposes. It is also to be noted, many times the vertical displacement at the load application points of the global internal forces (shear force, bending moment) fits for evaluation. The vertical axis shows the load factor, representing the combined loading situation with one measure. In

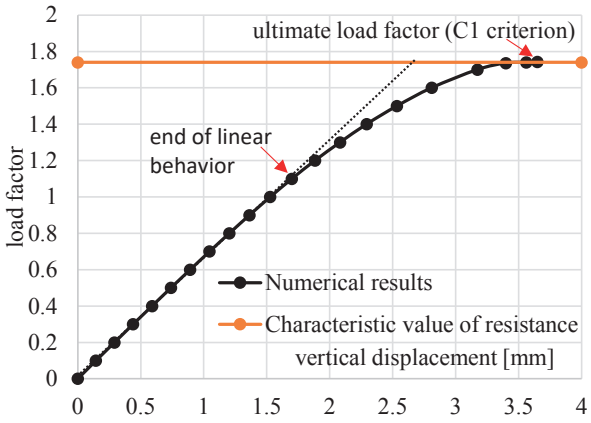

Fig. 16 Calculated load-deformation path

the current model load factor equal to 1.0 means the design value of internal forces calculated on the global numerical model (considering partial safety factors).

The highest point of the load-deformation path (R_{GMNIA}) is equal to a load factor of 1.734. It is checked, the maximum plastic strains at the ultimate load level does not reach 5 %, which is the predefined maximum allowed value for welded plated structures. The characteristic buckling resistance ($R_{b,k}$) should be determined by modifying the resistance assessed from a GMNIA analysis (R_{GMNIA}) according to the model factor γFE.

$$R_{b,k} = \frac{R_{GMNIA}}{\gamma_{FE}} = \frac{1.734}{1.0} = 1.72 \tag{7}$$

The design buckling resistance ($R_{b,d}$) can be determined on the basis of the characteristic buckling resistance ($R_{b,k}$) divided by the partial safety factor (γ_{M1}) according to EN 1993-2 [13] as given by Eq. (8).

$$R_{b,d} = \frac{R_{b,k}}{\gamma_{M1}} = \frac{1.734}{1.10} = 1.58 \tag{8}$$

The design buckling resistance should be compared to the design value of the internal forces represented here by load factor equal to 1.0. It means the utilization ratio of the analyzed structure is 63 % in the critical loading situation.

5 Effect of failure mode and geometry on the imperfection sensitivity

Similar calculations as presented in Table 3 and Fig. 15 are also executed by changing the plate thicknesses, which significantly control the obtained failure mode. The thickness of the bottom plate and web plates are changed from 12 mm to 30 mm. All the other geometrical properties of the model and applied internal forces are kept unchanged, so the girder is loaded by combination of bending

moment, shear, and transverse force (M-V-F interaction). The obtained ultimate load factors are divided by the minimum load factor taken from the 28 different imperfection combinations and the results are presented in Fig. 17. Imperfection ID-s refer to the same imperfection combinations as given in Table 3.

Diagram shows the trends obtained for the global and local imperfections are different than in the previous case. The main difference is that ratio of the maximum and minimum values is 25 %, while it was only 14.5 % in the previous case. It means, that the model having 30 mm plate thickness has larger imperfection sensitivity. Detailed evaluation of the results shows this fact is not related to the buckling behavior of the stiffened plate, but it comes from their sensitivity to different imperfection combinations. The previous model was not sensitive for the mixed direction of the global imperfections applied on the web and bottom plates. However, the modified model has slightly different failure mode (combined failure of the web and bottom plate), and the imperfection directions have larger effect resulting in larger imperfection sensitivity to the model. These results also confirm the direction of local imperfection has no significant effect on the ultimate load, but the direction of the global imperfection has crucial effect. Results prove different failure modes can have different sensitivity to imperfection combinations, therefore they cannot be neglected and supplemented by a single reduction factor.

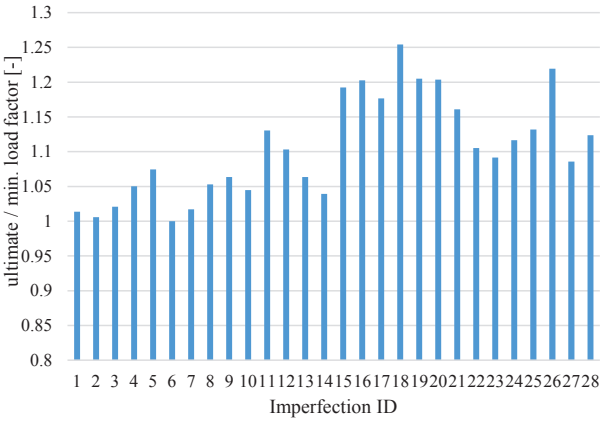

Fig. 17 Effect of imperfection combinations on ultimate load factor

6 Summary

In the current paper the application of FEM based design approach is introduced via a benchmark example on a steel box-section girder subjected by M-V-F interaction. The static check of the structure against combined loading situation and interacting stability phenomenon is presented. Specialties of the FEM based design process according to the recently developed new prEN 1993-1-14 are introduced, with special attention regarding material models, imperfections, imperfection combinations, validation and verification and result evaluation strategies.

Different methods on imperfection application are presented and their results on the resistance is evaluated. Different imperfections representing different stability problems are also combined using imperfection combination rules. Effect of the different imperfection combinations on the ultimate behavior and resistance is evaluated and conclusions are drawn for the analyzed structure type. Application of the modelling steps, validation and verification process are also presented, which were previously not completely regulated by standard provisions.

The calculation results presented in the paper are similar to classical worked examples for FEM based design, which can give clear application guidelines to designers, how to use and how to interpret the design rules of the prEN 1993-1-14. Another aspect giving scientific novelty to the paper is that the new code gives some choices to designers in the modelling process (e.g., applied material model, imperfections and imperfections combinations, value of the model factor γ_{FE}), the effect and impact of these choices are presented and evaluated in the current paper.

References

[1] CEN "EN 1993-1-5:2005, Eurocode 3: Design of steel structures, Part 1-5: Plated Structural elements", European Committee for Standardization, Brussels, Belgium, 2006.

[2] Braun, B. "Stability of steel plates under combined loading", PhD Thesis, Institute for Structural Design, University of Stuttgart, 2010. [online] Available at: https://d-nb.info/1009711792/34

[3] Graciano, C., Ayestarán, A. "Steel plate girders under combined patch loading, bending and shear", Journal of Constructional Steel Research, 80, pp. 202–212, 2013. https://doi.org/10.1016/j.jcsr.2012.09.018

[4] Kövesdi, B., Alcaine, J., Dunai, L., Mirambell, E., Braun, B., Kuhlmann, U. "Interaction behavior of steel I-girders Part I: Longitudinally unstiffened girders", Journal of Constructional Steel Research, 103, pp. 327–343, 2014. https://doi.org/10.1016/j.jcsr.2014.06.018

[5] Kövesdi, B., Alcaine, J., Dunai, L., Mirambell, E., Braun, B., Kuhlmann, U. "Interaction behavior of steel I-girders; part II: Longitudinally stiffened girders", Journal of Constructional Steel Research, 103, pp. 344–353, 2014. https://doi.org/10.1016/j.jcsr.2014.06.017

[6] CEN "prEN 1993-1-14:2020, Eurocode 3: Design of steel structures, Part 1-14: Design assisted by Finite element analysis", European Committee for Standardization, Brussels, Belgium, 2020.

[7] CEN "EN 1993-1-6:2005, Eurocode 3: Design of steel structures, Part 1-6: Strength and stability of shell structures", European Committee for Standardization, Brussels, Belgium, 2006.

[8] ANSYS "ANSYS® (v17.2)", [computer program] Available at: https://www.ansys.com/

[9] Gardner, L., Yun, X., Fieber, A., Macorini, L. "Steel Design by Advanced Analysis: Material Modeling and Strain Limits", Engineering, 5, pp. 243–249, 2019. https://doi.org/10.1016/j.eng.2018.11.026

[10] Budaházy, V., Dunai, L. "Parameter-refreshed Chaboche model for mild steel cyclic plasticity behaviour", Periodica Polytechnica Civil Engineering, 57(2), pp. 139–155, 2013. https://doi.org/10.3311/PPci.7170

[11] Timmers, R., Schwienbacher, M., Lang, R., Lener, G. "Proposal and validation of a simplified numerical buckling check for stiffened plated elements", presented at Eighth International Conference on Thin-Walled Structures, ICTWS 2018, Lisbon, Portugal, July, 24–27, 2018.

[12] Kövesdi, B., Dunai, L. "Determination of the patch loading resistance of girders with corrugated webs using nonlinear finite element analysis", Computers & Structures, 89, pp. 2010–2019, 2011. https://doi.org/10.1016/j.compstruc.2011.05.014

[13] CEN "EN 1993-2:2006, Eurocode 3: Design of steel structures, Part 2: Steel bridges", European Committee for Standardization, Brussels, Belgium, 2006.